

In Vitro Oxidative Metabolism of 6-Mercaptopurine in Human Liver: Insights into the Role of the Molybdoflavoenzymes Aldehyde Oxidase, Xanthine Oxidase, and Xanthine Dehydrogenase[§]

Kanika V. Choughule, Carlo Barnaba, Carolyn A. Joswig-Jones, and Jeffrey P. Jones

Department of Chemistry, Washington State University, Pullman, Washington

Received March 13, 2014; accepted May 13, 2014

ABSTRACT

Anticancer agent 6-mercaptopurine (6MP) has been in use since 1953 for the treatment of childhood acute lymphoblastic leukemia (ALL) and inflammatory bowel disease. Despite being available for 60 years, several aspects of 6MP drug metabolism and pharmacokinetics in humans are unknown. Molybdoflavoenzymes such as aldehyde oxidase (AO) and xanthine oxidase (XO) have previously been implicated in the metabolism of this drug. In this study, we investigated the *in vitro* metabolism of 6MP to 6-thiouric acid (6TUA) in pooled human liver cytosol. We discovered that 6MP is metabolized to 6TUA through sequential metabolism via the 6-thioxanthine (6TX) intermediate. The role of human AO and XO in the metabolism of 6MP was established using the specific inhibitors raloxifene and febuxostat.

Both AO and XO were involved in the metabolism of the 6TX intermediate, whereas only XO was responsible for the conversion of 6TX to 6TUA. These findings were further confirmed using purified human AO and *Escherichia coli* lysate containing expressed recombinant human XO. Xanthine dehydrogenase (XDH), which belongs to the family of xanthine oxidoreductases and preferentially reduces nicotinamide adenine dinucleotide (NAD⁺), was shown to contribute to the overall production of the 6TX intermediate as well as the final product 6TUA in the presence of NAD⁺ in human liver cytosol. In conclusion, we present evidence that three enzymes, AO, XO, and XDH, contribute to the production of 6TX intermediate, whereas only XO and XDH are involved in the conversion of 6TX to 6TUA in pooled HLC.

Introduction

6-Mercaptopurine (6MP) is a thiopurine drug with antitumor activity that has been in use as a remission-inducing agent for the treatment of childhood acute lymphoblastic leukemia (Burchenal et al., 1953). It has also been used as an immunosuppressive agent in combination with its prodrug, azathioprine, for the treatment of inflammatory bowel disease such as ulcerative colitis and Crohn's disease (Nielsen et al., 2001). 6MP is structurally related to endogenous purine bases such as adenine, guanine, and hypoxanthine, and hence is metabolized by enzyme systems and pathways that metabolize endogenous purines (Aarbakke et al., 1997). Phosphoribosylation, oxidation, and methylation are the major metabolic pathways of 6MP metabolism (Fig. 1). Phosphoribosylation is an anabolic pathway that results in the production of active metabolites that exert the antitumor effect of 6MP by interfering with purine ribonucleotide synthesis. As opposed to phosphoribosylation, oxidation and methylation are catabolic pathways that produce inactive metabolites. It has been known that 6MP is converted to methylmercaptopurine (MeMP) by the action of thiopurine methyltransferase by a pathway that is almost exclusive for thiopurines (Giverhaug et al., 1999). Oxidative metabolism of 6MP results in 6-thiouric acid (6TUA), 6-thioxanthine (6TX), 8-oxo-6-mercaptopurine (8-oxo-6MP), and 6-methylmercapto-8-hydroxypurine (6Me-8OH-MP)

in vivo (Keuzenkamp-Jansen et al., 1996; Rowland et al., 1999). There is contradictory evidence on whether 6MP is converted to 6TUA via 6TX or 8-oxo-6MP *in vivo*. Early pharmacokinetic studies revealed that this drug was initially oxidized to 8-oxo-6-mercaptopurine before being converted to 6-thiouric acid (Bergmann and Ungar, 1960; Elion, 1967; Van Scoick et al., 1985). However, Zimm et al. (1984) identified 6-thioxanthine in urine of patients dosed with 6MP and proposed that this metabolite could also be an intermediate in the formation of 6-thiouric acid. Human xanthine oxidase (XO) and aldehyde oxidase (AO) are very closely related molybdoflavoenzymes that have a high degree of amino acid sequence identity, require the same cofactors (Garattini et al., 2003), and share a similar mechanism of action (Alfaro and Jones, 2008). However, they still differ remarkably in their substrate specificities (Garattini and Terao, 2012). Conversion of 6MP to 6TUA has been attributed to the activity of these molybdoflavoenzymes. 6MP has a low oral bioavailability because of extensive first pass metabolism by hepatic and intestinal enzymes. It is believed that the drug is rapidly oxidized to its major *in vivo* metabolite, 6-thiouric acid, by the action of XO in the liver and intestine. Administration of 6MP along with XO inhibitors have resulted in an increase in the bioavailability of this drug (Balis et al., 1987; Giverhaug et al., 1999). Apart from this, 6MP is also converted to 6TUA by calf liver XO, bovine milk XO (Krenitsky et al., 1972), and rabbit liver AO (Hall and Krenitsky, 1986). However, the contribution of AO/XO in the conversion of 6MP to its intermediate and subsequently to 6TUA in humans is largely unknown. Evidence by Rashidi et al. (2007) suggests that 6MP is sequentially metabolized to produce 6TUA through the

This work was supported by a grant from the National Institutes of Health [GM100874 (to J.P.J.)].

dx.doi.org/10.1124/dmd.114.058107.

[§]This article has supplemental material available at dmd.aspetjournals.org.

ABBREVIATIONS: 6MP, 6-mercaptopurine; 6TUA, 6-thiouric acid; 6TX, 6-thioxanthine; AO, aldehyde oxidase; HLC, human liver cytosol; HPLC, high-performance liquid chromatography; LB, lysogeny broth; LC, liquid chromatography; MS/MS, tandem mass spectrometry; NAD, nicotinamide adenine dinucleotide; XDH, xanthine dehydrogenase; XO, xanthine oxidase; XOR, xanthine oxidoreductase.

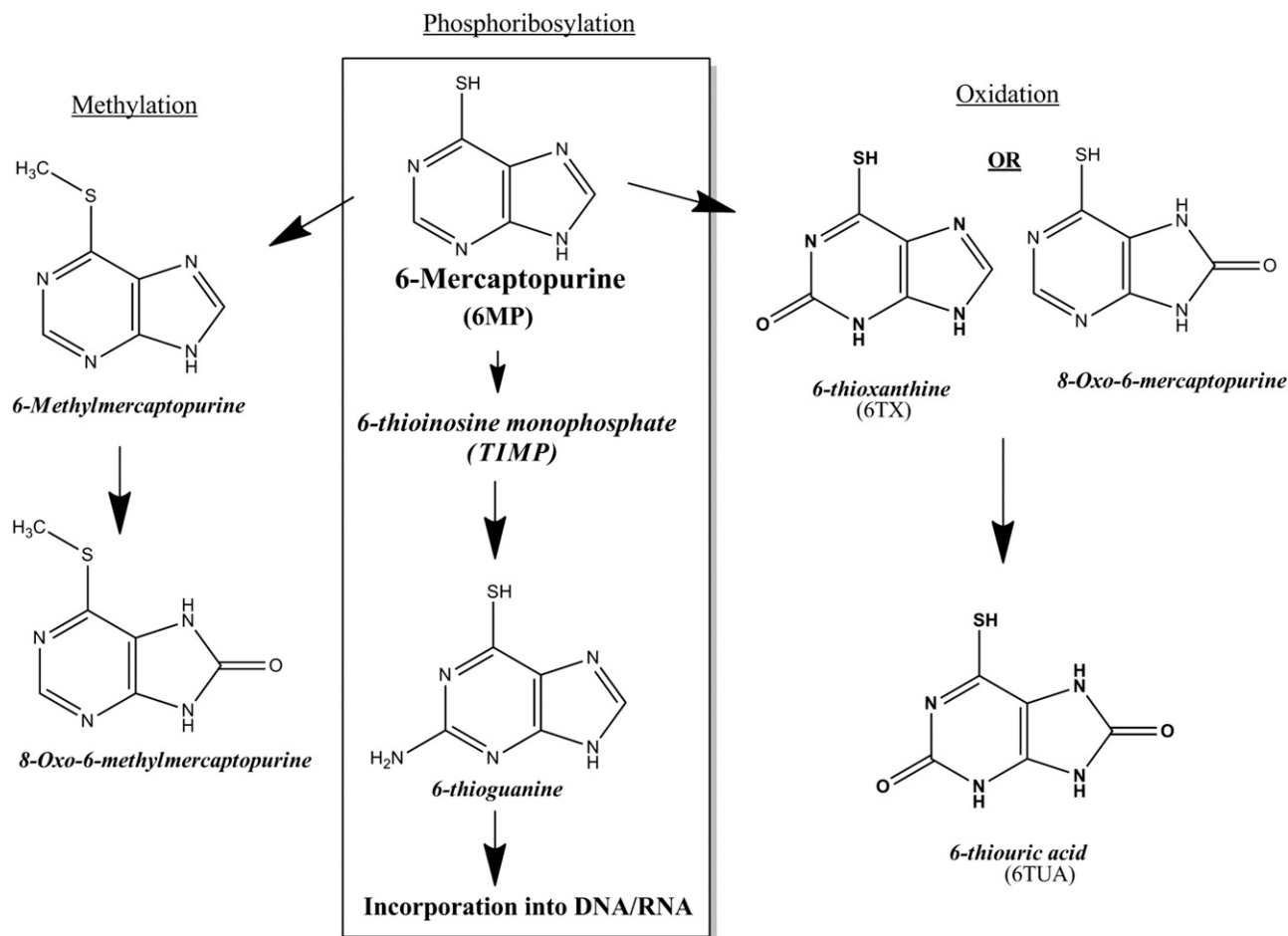


Fig. 1. Reaction scheme showing metabolites of 6-Mercaptopurine formed by phosphoribosylation (anabolic), methylation and oxidation (catabolic) pathways.

intermediate metabolite 6TX in partially purified guinea pig liver. Rashidi et al. also demonstrated that 6MP is metabolized to 6TX exclusively by XO and subsequently converted to 6TUA by a concerted action of XO and AO. One caveat to bear in mind is that all of these in vitro experiments were performed using AO/XO from nonhuman sources. Major species differences have already been reported for several compounds metabolized by AO and hence extrapolation of pharmacokinetic data from other mammalian species to humans is not advisable (Choughule et al., 2013; Dalvie et al., 2013). Moreover, mammalian xanthine oxidoreductase (XOR) exists in two interconvertible forms, xanthine oxidase (XO) and xanthine dehydrogenase (XDH). XDH preferentially reduces nicotinamide adenine dinucleotide (NAD^+) and predominates in vivo, while XO cannot reduce NAD^+ and prefers molecular oxygen as an electron acceptor (Harrison, 2002). It has already been established that XO plays a role in the metabolism of 6MP. However, the contribution of XDH to the metabolism of this thiopurine drug still remains largely unknown.

To understand the in vitro oxidative metabolism of this well established anticancer drug, we investigated the in vitro metabolism of 6MP to 6TUA via the 6TX intermediate in pooled human liver cytosol. The roles of XO and AO were explored using specific inhibitors raloxifene and febuxostat. We confirmed the roles by using purified human AO and *Escherichia coli* lysate containing expressed recombinant human XO. Finally, we assessed the metabolism in the presence and absence of NAD^+ to determine the role of XDH to the overall metabolism of 6MP and 6TX.

Materials and Methods

6-Mercaptopurine was purchased from Sigma-Aldrich (St. Louis, MO), whereas 6-thioxanthine and 6-thiouric acid were purchased from Toronto Research Chemicals (Toronto, ON, Canada). Febuxostat was kindly donated by Dr. Eric Kelley from University of Pittsburgh (Pittsburgh, PA). Raloxifene was purchased from Enzo Life Sciences (Farmingdale, NY). Sequence grade trypsin was acquired from Promega (Madison, WI). Pooled mixed-gender human liver samples ($n = 8$) devoid of allopurinol were obtained from St Jude's Children's Hospital human liver bank (Barr et al., 2014). The samples were prepared and stored as described in (Barr et al., 2014). Table 1 contains information on the demographics of the liver samples used to prepare cytosol. Plasmid pTrc99A containing gene encoding for human XO was kindly provided by Tomohiro Matsumura from Nippon Medical School (Tokyo, Japan).

Expression of Recombinant Human XOR in TP1000 Cells. Human XOR containing plasmid DNA (10 ng) was transformed into TP1000 cells (a gift from John Enemark's laboratory, University of Arizona). Transformants were plated on lysogeny broth (LB) agar plates containing 100 $\mu\text{g}/\text{ml}$ ampicillin and grown overnight at 37°C. A single colony was used to inoculate 100 ml of LB containing 100 $\mu\text{g}/\text{ml}$ ampicillin. Cell stocks were prepared in 15% glycerol and stored at -80°C until further use.

For expression of human XOR, glycerol stocks of TP1000 cells containing plasmid pRTC99A encoding human XOR were plated onto LB agarose plates containing 100 $\mu\text{g}/\text{ml}$ ampicillin. A single colony was picked and grown overnight at 30°C in 100 ml LB containing 100 $\mu\text{g}/\text{ml}$ ampicillin and 50 μM sodium molybdate. A 10-ml aliquot of the culture was used to inoculate 500 ml fresh LB broth with 100 $\mu\text{g}/\text{ml}$ ampicillin and 50 μM sodium molybdate. Cultures were grown at 37°C and 250 rpm for 2 hours until an absorbance of 1 at 600 nm was reached. Isopropyl β -D-thiogalactoside (IPTG) at a final concentration of 1 mM was

TABLE 1

Demographics of individual liver samples pooled to generate human liver cytosol used in this study

Liver	Sex	Age	Disease History
1	Female	69	Hepatoma
2	Male	62	Colorectal cancer, metastasis
3	Female	68	Colorectal cancer, metastasis
4	Female	63	Cholangio carcinoma
5	Female	60	Colorectal cancer, metastasis
6	Female	70	Colorectal cancer, metastasis
7	Female	24	No information given
8	Male	57	Colorectal cancer, metastasis

used to induce cells, which were then allowed to continue growing at room temperature for 24 hours at 150 rpm. Cells were harvested by centrifugation at 3500g at 4°C for 30 minutes in a swinging bucket rotor (Allegra 6R centrifuge; Beckman Coulter, Pasadena, CA). Cell paste was collected and resuspended in equal volumes of 1 g of paste to 1 ml of buffer (100 mM potassium phosphate buffer, pH 7.4). Cell suspension was lysed by adding lysozyme (5 mg/ml), MgCl₂ (28.6 μg/ml), RNase, and DNase (10 μg/ml of each) followed by incubation at 4°C for 60 minutes. The cell suspension was then disrupted by sonication and subsequently subjected to centrifugation at 100,000g for 40 minutes at 4°C. Supernatant containing recombinant human XO was collected and stored at -80°C until further use.

Expression of Human AOX1 and Subsequent Protein Purification. The method of human AOX1 gene expression and purification previously developed in our laboratory was used in this study for the preparation of purified human AO (Alfaro et al., 2009). Human AOX1 was overexpressed as a fusion protein with an N-terminal hexa-His tag in TP1000 cells. Partial purification was achieved by lysing the cells and passing the lysate through a 1-ml HiTrap Chelating HP column (GE Healthcare, Little Chalfont, Buckinghamshire, UK). The purified protein was subsequently dialyzed into 100 mM potassium phosphate buffer, pH 7.4, and snap frozen in liquid nitrogen and stored at -80°C.

Quantitation of Purified AO by High-Performance Liquid Chromatography–Tandem Mass Spectrometry with Electrospray Interface. The amount of AO in purified samples was quantified using a technique previously developed in our laboratory (Barr et al., 2013). A deuterium-labeled synthetic peptide standard was used to determine the amount of AO in purified samples. A sample consisting of 25 μl of purified AO (1.5 μM) was mixed with an equal volume of denaturing solution containing 8 M urea and 2 mM dithiothreitol and incubated at 60°C for 60 minutes. Sodium bicarbonate buffer (25 mM, pH 8.4) containing 100 nM internal standard peptide was added to the mixture so that the final reaction volume was 250 μl. Ten milliliters of 20-μg trypsin was added to the reaction mixture and incubated for 15 hours at 37°C. The reaction was quenched by adding 50 μl of 50% v/v trifluoroacetic acid (TFA) in water to 200 μl of reaction mixture. The samples were vortexed and centrifuged at 1460g for 10 minutes and analyzed using high-performance liquid chromatography–tandem mass spectrometry (HPLC-MS/MS). The native peptide and hence the amount of purified AO in a sample was quantified by comparing its MS peak area to the peak area of the internal standard peptide of a known concentration.

Incubation Conditions. The incubation mixture consisted of substrates 6MP or 6TX at a final concentration in the range of 10–1000 μM and 0.1–200 μM, respectively, in 25 mM potassium phosphate buffer (pH 7.4) containing 0.1 mM EDTA. The final concentration of dimethylsulfoxide was 0.5% (v/v). For the inhibition experiments, a substrate concentration of 100 μM was used. Inhibitors raloxifene and febuxostat were used at a final concentration of 1 μM. The substrate and inhibitor stocks were made up so that the total concentration of dimethylsulfoxide in the reaction mixture was 1.5% (v/v). All incubations for 6TX and 6TUA formation were allowed to proceed at 37°C for 15 and 30 minutes, respectively. The formation of 6TX was observed to be linear with respect to time for 15 minutes and 6TUA for more than 30 minutes. The reaction was initiated by addition of pooled human liver cytosol (HLC) at a final concentration of 0.5 or 1 mg/ml and a known concentration of purified human AO and human XO lysate. The final reaction volume was 80 μl. The reaction was quenched by the addition of 20 μl of 1 M formic acid containing

1 μM 3,5 dibromo-4-hydroxybenzoic acid as internal standard. The samples were then centrifuged at 5000 rpm for 10 minutes in an Eppendorf centrifuge 5415D and the supernatant was collected for analysis.

HPLC-MS/MS Assays. The samples were analyzed using an 1100 series HPLC system (Agilent Technologies, Santa Clara, CA) coupled to a API4000 tandem mass spectrometry system (Applied Biosystems/MDS Sciex, Foster City, CA) on a turbospray interface (ESI) operating in negative ion mode. Chromatography was performed on a Zorbax Eclipse XDB-C8 column (4.6 × 150 mm; 5 μm; Agilent Technologies, Santa Clara, CA). Mobile phase A consisted of 0.05% formic acid and 0.2% acetic acid in water and mobile phase B contained 90% acetonitrile, 9.9% water, and 0.1% formic acid. The column was first equilibrated with 99% mobile phase A for 3 minutes. Chromatographic separation was achieved using a linear gradient to 25% mobile phase A over the next 1.5 minutes. Mobile phase A was then held constant for the next 1.5 minutes before a linear gradient back to 99% mobile phase A was achieved over a period of 1 minute. Finally, the column was re-equilibrated to starting conditions over the next 1 minute. The entire chromatographic assay was performed over 8 minutes per sample with a constant flow rate of 800 μl/min. The retention times for 6-thioxanthine, 6-thiouric acid, and the internal standard were 6.2, 4.5, and 6.8 minutes, respectively (see Supplemental Fig. 1). The optimized mass spectrometer tune parameters for 6TX and 6TUA were as follows: collision gas, 10; curtain gas, 30; ion source gas 1, 50; ion source gas 2, 30; ion spray voltage, 4500; desolvation temperature, 450; declustering potential, 70; entrance potential, 15; collision energy, 30; collision cell exit potential, 2. The analytes, 6TX, 6TUA, and the internal standard, were detected using multiple reaction monitoring mode by monitoring the *m/z* transition from 167.1 to 133.4, 183.0 to 140.2, and 294.8 to 251, respectively. Quantitation of the product was achieved by comparison with a standard curve ranging from 1 nM to 10 μM for 6TX and 0.1 to 10 μM for 6TUA.

Data Analysis. Experimental data were fitted to appropriate nonlinear regression models using GraphPad Prism (version 4.03; GraphPad Software Inc., San Diego, CA).

Michaelis-Menten model:

$$V = \frac{V_{max}[S]}{K_m + [S]} \quad (1)$$

Substrate inhibition model:

$$V = \frac{V_{max}[S]}{K_m + [S] \left(1 + \frac{[S]}{K_i}\right)} \quad (2)$$

where *V* is the reaction velocity, [*S*] is the substrate concentration, *V*_{max} is the maximum reaction velocity, *K*_m is the Michaelis-Menten constant, and *K*_i is the inhibition constant for the substrate.

Visual inspection of the velocity curve inflection (Figs. 3A and 5A), as well as the biphasic nature of the kinetic displayed by Eadie-Hofstee plot (Fig. 3Ai), led us to fit the data to the equation for two or more enzymes catalyzing the same reaction. This kinetic approach considers the total velocity as the sum of the contribution by each enzyme (Segel, 1993):

$$V = \left\{ \frac{V_{max1}[S]}{K_{m1} + [S]} \right\} + \left\{ \frac{V_{max2}[S]}{K_{m2} + [S]} \right\} \quad (3)$$

Here, *V*_{max1} is the lower *V*_{max}, *V*_{max2} is the higher *V*_{max}, *K*_{m1} is the lower *K*_m and *K*_{m2} is the higher *K*_m. Since nonlinear regression methods failed to converge, Lineweaver-Burk plots were used to estimate the kinetic constants *V*_{max} and *K*_m for biphasic reactions. Reciprocal plots generated using data points from the region below the first inflection of the biphasic curve were used to obtain *K*_{m1} and *V*_{max1}, and points above the first inflection were used to predict *K*_{m2} and *V*_{max2}.

Results and Discussion

Metabolism of 6MP to 6TUA by the molybdenum hydroxylases requires two sequential oxidations. Evidence in the literature suggests that 6MP can form 6TUA either via 6TX or 8-OH-6MP as an intermediate *in vivo* in humans, but the enzymes responsible for the reactions are not known (Bergmann and Ungar, 1960; Zimm et al.,

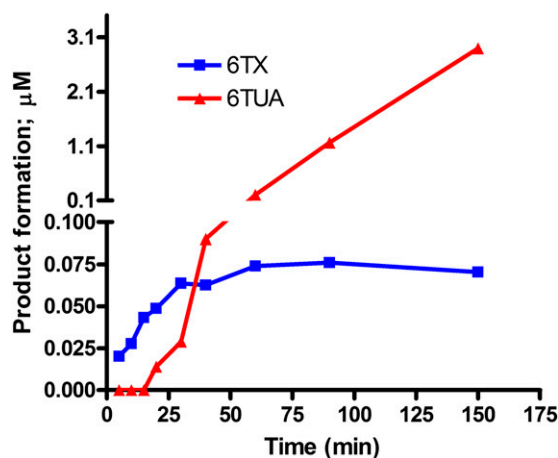


Fig. 2. Dynamics of the formation of the intermediate, 6TX and the final product, 6TUA in human liver cytosol over a period of 150 minutes.

1984; Van Scoik et al., 1985) (see Fig. 1). Studies using cow XO and guinea pig AO concluded that oxidation to the 6TX intermediate was mediated solely by XO. The second step was found to be mediated by both guinea pig AO and cow XO (Rashidi et al., 2007). Given that many studies have shown that animal models are poor predictor of molybdenum oxidase activity we decided to explore the *in vitro*

metabolism with human XO and AO (Sahi et al., 2008; Choughule et al., 2013; Dalvie et al., 2013).

We initially explored the time course of 6MP metabolism by monitoring the production of the intermediate 6TX and the final product 6TUA in pooled human liver cytosol. The results are shown in Fig. 2. The intermediate 6TX is formed at a relatively linear rate for almost 25 minutes. Between 25 and 40 minutes the intermediate reaches steady-state concentrations. The final product is formed after an initial lag of about 25–40 minutes and produced in a linear fashion after the intermediate 6TX reached steady-state. These results are consistent with sequential oxidation with release of the intermediate prior to the second step. Thus, the intermediate 6TX must rebind to the enzyme and does not simply reorient in the active site. Due to the unavailability of the 8-OH-6MP metabolite standard, it was not possible to investigate the contribution of this intermediate. However, a recent crystallography study has shown that both 6MP and hypoxanthine bind in two orientations that could lead to either oxidation on the five-membered or six-membered ring of either substrate (Cao et al., 2010). While 6MP metabolism was not explored, this study concluded that xanthine (oxidation on the six-membered ring) was the major intermediate of hypoxanthine oxidation and that oxidation on the five-membered ring was not observed. Thus, the formation of 6TX (oxidation on the six-membered ring) is consistent with the results for hypoxanthine oxidation. Furthermore, the correlation between steady-state 6TX levels and 6TUA linear rates support 6TX as the major intermediate, or that 6TX and 8-OH-6MP are formed with nearly identical kinetics.

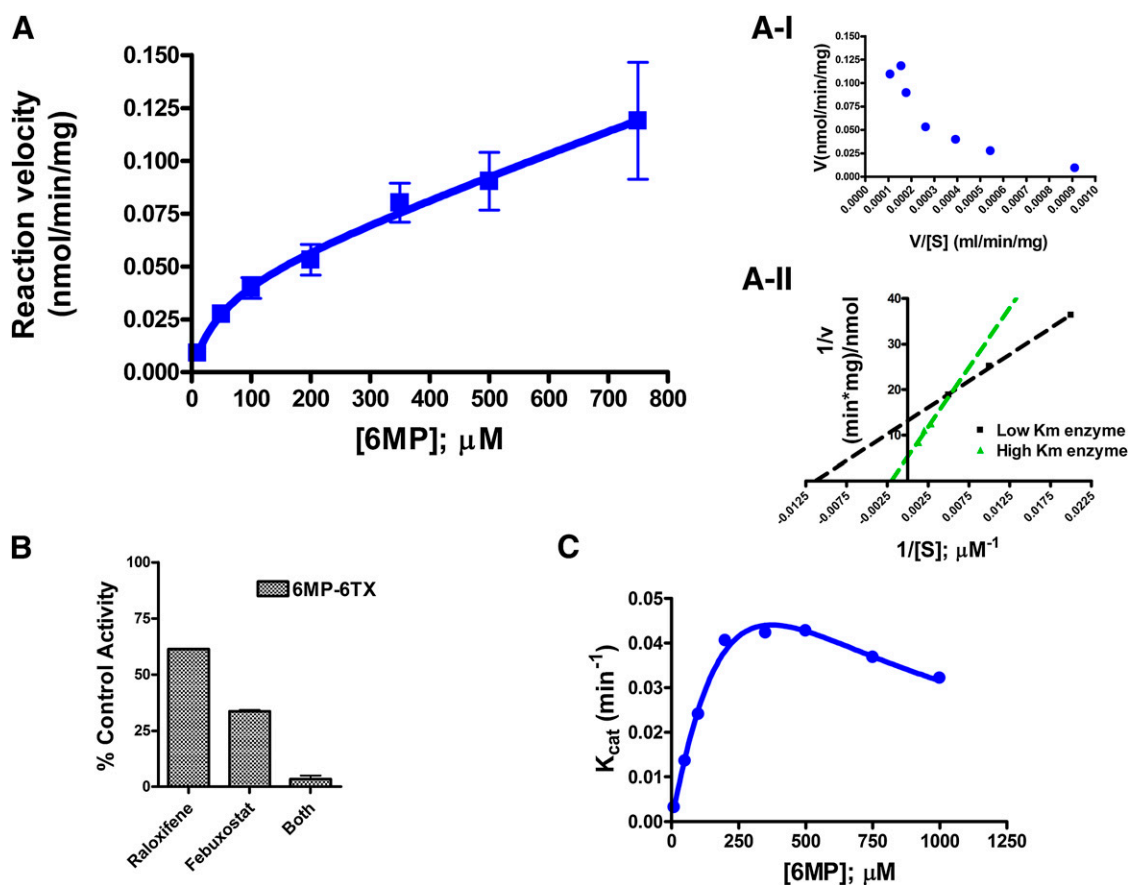


Fig. 3. (A) Biphasic curve showing the formation of the intermediate 6TX from 6MP in human liver cytosol in the absence of NAD^+ . Points represent mean and error bars show standard error for triplicate experiments. Shown as an inset are Eadie Hofstee plot (A-I) and Lineweaver-Burke plot (A-II) representation of the same data. Points represent an average of triplicate experiments. (B) Inhibition of 6TX formation from 100 μM 6MP by AO specific inhibitor raloxifene (1 μM) and XO specific inhibitor febuxostat (1 μM) in HLC. Each reaction was performed in duplicate and values are expressed as percentage activity relative to the activity observed in the control (No inhibitor added). Error bars represent \pm SEM. (C) Saturation plot for 6MP oxidation to 6TX in purified human AO showing K_{cat} (min^{-1}) versus substrate concentration. Data are fit to a substrate inhibition model and are an average of duplicate experiments.

TABLE 2

Enzyme kinetic parameters for the conversion of 6-mercaptopurine to 6-thioxanthine and 6-thioxanthine to 6-thiouric acid in pooled human liver cytosol in the presence and absence of NAD⁺

Data are representative of at least duplicate measurements \pm S.E.M.

Reaction	Source	Enzyme Kinetics	V_{\max}		K_m	
			$V_{\max 1}$	$V_{\max 2}$	K_{m1}	K_{m2}
			nmol/min per milligram		μM	
6MP \rightarrow 6TX	HLC (-NAD)	Biphasic	0.08 \pm 0.00	0.2 \pm 0.1	88.2 \pm 4.4	500 \pm 188
	HLC (+NAD)	Biphasic	0.2 \pm 0.01	0.3 \pm 0.1	83.4 \pm 2.9	339 \pm 169
6TX \rightarrow 6TUA	HLC (-NAD)	Michaelis-Menten	7.2 \pm 0.2	NA	3.0 \pm 0.4	NA
	HLC (+NAD)	Michaelis-Menten	15.5 \pm 0.7	NA	8.0 \pm 1.6	NA

With 6TX established as an intermediate in the formation of 6TUA, the next step was to determine the kinetics of the 6TX formation. Fig. 3A shows that biphasic kinetics was observed for 6TX formation. The Eadie-Hofstee plot shown in Fig. 3Ai, also displays a biphasic profile. Biphasic profiles are generally a result of a single enzyme in possession of a low- and a high-affinity catalytic binding site or two distinct enzymes involved in the biotransformation of a single substrate, one having low and the other having high affinity toward the substrate (Hutzler and Tracy, 2002). After using Lineweaver-Burke plots to fit the data (Fig. 3Aii), $V_{\max 1}/V_{\max 2}$ and K_{m1}/K_{m2} were estimated to be 0.08/0.2 nmol/min per milligram and 88/500 μM , respectively (Table 2). Thus, one high-affinity enzyme/active site and one high-capacity enzyme/active site is involved in metabolism to the 6TX intermediate, but the identity of the specific enzymes are unknown.

Specific inhibitors were used to address whether both AO and XO are involved in 6TX production. Raloxifene and febuxostat specifically inhibit drug metabolism by AO and XO, respectively, at concentrations up to 1 μM . (Obach, 2004; Barr and Jones, 2013; Weidert et al., 2014). Raloxifene inhibited the formation of 6TX by approximately 39%, whereas febuxostat demonstrated 67% inhibition (Fig. 3B). When both inhibitors were used in the same incubation they inhibited 97% of the formation of 6TX (Fig. 3B). Neither raloxifene nor febuxostat independently resulted in complete inhibition of 6TX production, implying that both AO and XO are involved in the generation of this intermediate metabolite. (Table 2).

To identify the high- and low- K_m enzyme, 6MP was incubated with either purified recombinant human aldehyde oxidase or *E. coli* cell lysate containing recombinant human xanthine oxidase. Purified human AO metabolized 6MP to 6TX and showed substrate inhibition kinetics with a K_{cat} of 0.2 minute^{-1} and a K_m of 572 μM (Fig. 3C). The K_m value of 572 μM obtained here (Table 3) is not significantly different from the K_{m2} value of 500 μM reported for 6TX formation in human liver cytosol above and hence it is probable that AO is the high- K_m enzyme associated with 6TX formation in human liver cytosol. This also means that XO is the likely low- K_m enzyme associated with this reaction. *Escherichia coli* lysate containing human

XO also converted 6MP to 6TX, but since the enzyme levels are very low in the unpurified lysate, it was not possible to perform saturation kinetics and subsequently obtain a K_m for this reaction for comparison with purified human AO. Thus, it appears that unlike guinea pig AO, human AO mediates the formation of 6TX, while both human and cow XO can also mediate this reaction.

Unlike 6TX formation, which followed biphasic kinetics, Michaelis-Menten kinetics were observed for the conversion of the intermediate 6TX to final product 6TUA in HLC. This indicates that a single enzyme, or more than one enzyme with similar K_m values, were involved in the catalysis of this step (Fig. 4A). Inhibition experiments with raloxifene indicated that AO was not involved in the conversion of this intermediate to the final product. Raloxifene inhibited only 9% of 6TUA formation, whereas the XO inhibitor febuxostat almost completely inhibited 6TUA formation from 6TX (Fig. 4B). In addition to this, purified human AO did not turn over 6TX to produce 6TUA but *E. coli* lysate containing expressed human XO converted 6TX to 6TUA following Michaelis-Menten kinetics (Fig. 4C). These results underpin the importance of XO in the metabolism of the intermediate to the final product and the absence of AO contribution to this step. This is again in contrast with the 6TX metabolism by guinea pig AO and cow XO (Rashidi et al., 2007), both of which catalyze the reaction. Interestingly, human liver cytosol has a higher V_{\max} and a lower K_m value of 3 μM than the *E. coli*-expressed enzyme (K_m , 30 μM) (Table 3). Given the uncertainty in the protein concentration of XO, the rate differences between the cytosolic XO and the expressed XO cannot be explained. However, it is surprising that the K_m values are different for the two enzyme systems. One possibility is that the human liver cytosol may have a significant amount of xanthine dehydrogenase (XDH) as well as XO.

To assess the contribution, if any, of XDH to the formation of 6TUA from 6TX, we performed kinetic experiments on human liver cytosol in the presence of NAD⁺. The kinetics of 6TUA formation from 6TX in the presence of NAD⁺ showed Michaelis-Menten kinetics with a doubling of V_{\max} from 7 to 15 nmol/min per milligram relative to no NAD⁺ (Fig. 5A). An increase in the K_m value from 3 to 8 μM was observed in the presence

TABLE 3

Enzyme kinetic parameters for the conversion of 6-mercaptopurine to 6-thioxanthine by purified recombinant human aldehyde oxidase and 6-thioxanthine to 6-thiouric acid by *E. coli* lysate containing recombinant human xanthine oxidase

Data are representative of at least duplicate measurements \pm S.E.M.

Reaction	Source	Enzyme Kinetics	V_{\max}		K_{cat}	K_m		K_i
			$V_{\max 1}$	$V_{\max 2}$		K_{m1}	K_{m2}	
			nmol/min per milligram			μM		
6MP \rightarrow 6TX	Purified human AO	Substrate Inhibition	NA	NA	0.2 \pm 0.0	572 \pm 172	NA	244 \pm 77
6TX \rightarrow 6TUA	Human XO containing <i>E. coli</i> lysate	Michaelis-Menten	NA	NA	NA	30 \pm 2	NA	NA

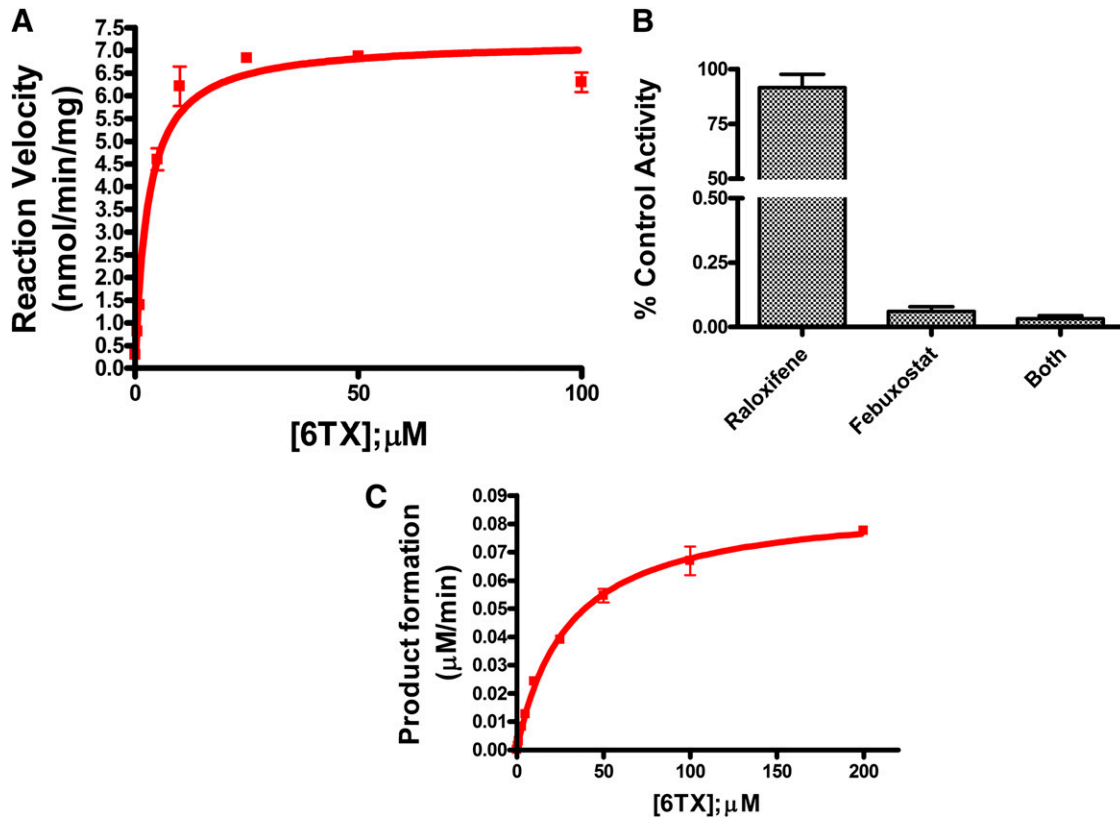


Fig. 4. (A) Michaelis-Menten kinetics for the formation of the final product 6TUA from the intermediate, 6TX in HLC and (C) lysate containing expressed human xanthine oxidase. Each experiment is an average of duplicate experiments (\pm SEM). (B) Inhibition of 6TUA formation from 100 μM 6TX in HLC by AO specific inhibitor raloxifene (1 μM) and XO specific inhibitor febuxostat (1 μM). Values are expressed as a percentage of activity relative to the activity observed in of the control (No inhibitor added). Data are an average of duplicate experiments \pm SEM.

of NAD^+ (Table 2). In short, adding NAD^+ to human liver cytosol did increase the rate of the reaction for the formation of the final product from the intermediate 6TX and can explain, at least in part, the difference

between the cytosolic and *E. coli*-expressed metabolism. This brings into question whether XDH may also play a role in the first rate-limiting step, the production of 6TX.

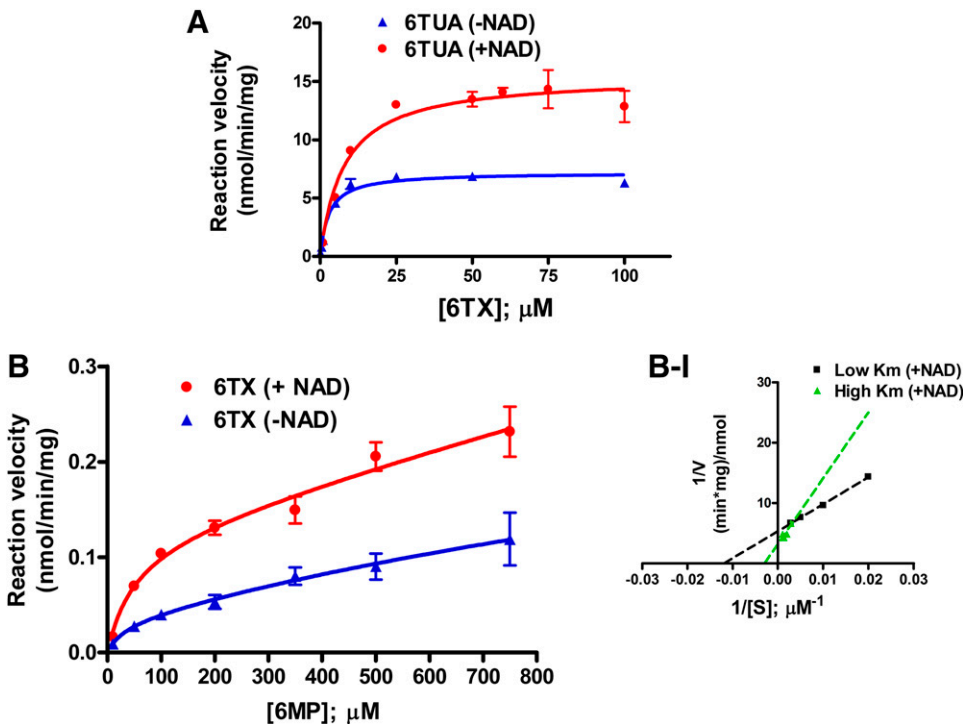


Fig. 5. (A) Metabolism of 6MP to form 6TUA from 6TX and (B) 6TX from 6MP in the presence (red) and absence (blue) of NAD^+ . HLC were used as a source of enzyme. Data points are an average of duplicate experiments \pm SEM. Shown as (B-I) is a Lineweaver-Burke plot of the same data used for estimation of kinetic parameters such as V_{max} and K_m .

In the presence of NAD^+ , kinetics of 6TX was still biphasic (Fig. 5B) but the kinetic parameters indicate a 2.5-fold increase in $V_{\max 1}$ value, with no significant difference in the $V_{\max 2}$ value (Table 2). (This would be expected since the second V_{\max} value has been assigned to AO.) Thus, it appears that XDH and XO contribute to the high-affinity reaction, while AO is responsible for the high-capacity reaction.

In conclusion, 6MP is converted to 6TUA via the intermediate 6TX. Three enzymes, AO, XO, and XDH, contribute to the production of the 6TX intermediate, whereas only XO and XDH are involved in the conversion of the intermediate to the final product. This is in direct contrast with studies using nonhuman tissue in which XO was found to be responsible for the first step, and both AO and XO were responsible for the second step. This study establishes the enzymes responsible for oxidation of 6MP, and underlines the potential problems associated with using other species to predict the role of human molybdenum oxidases.

Acknowledgments

The authors thank Dr. Tomohiro Matsumura at Nippon Medical School (Tokyo, Japan) for providing us with the plasmid pTrc99A containing the gene encoding human XO.

Authorship Contributions

Participated in research design: Choughule, Joswig-Jones, Jones.

Conducted experiments: Choughule, Joswig-Jones.

Performed data analysis: Choughule, Jones, Barnaba.

Wrote or contributed to the writing of the manuscript: Choughule, Barnaba, Jones.

References

- Aarbakke J, Janka-Schaub G, and Elion GB (1997) Thiopurine biology and pharmacology. *Trends Pharmacol Sci* **18**:3–7.
- Alfaro JF and Jones JP (2008) Studies on the mechanism of aldehyde oxidase and xanthine oxidase. *J Org Chem* **73**:9469–9472.
- Alfaro JF, Joswig-Jones CA, Ouyang W, Nichols J, Crouch GJ, and Jones JP (2009) Purification and mechanism of human aldehyde oxidase expressed in *Escherichia coli*. *Drug Metab Dispos* **37**:2393–2398.
- Balis FM, Holcenberg JS, Zimm S, Tubergen D, Collins JM, Murphy RF, Gilchrist GS, Hammond D, and Poplack DG (1987) The effect of methotrexate on the bioavailability of oral 6-mercaptopurine. *Clin Pharmacol Ther* **41**:384–387.
- Barr JT and Jones JP (2013) Evidence for substrate-dependent inhibition profiles for human liver aldehyde oxidase. *Drug Metab Dispos* **41**:24–29.
- Barr JT, Jones JP, Joswig-Jones CA, and Rock DA (2013) Absolute quantification of aldehyde oxidase protein in human liver using liquid chromatography-tandem mass spectrometry. *Mol Pharm* **10**:3842–3849.
- Barr JT, Choughule KV, Nepal S, Wong T, Chaudhry AS, Joswig-Jones CA, Zientek M, Strom SC, Schuetz EG, and Thummel KE, et al. (2014) Why do most human liver cytosol preparations lack xanthine oxidase activity? *Drug Metab Dispos* **42**:695–699.
- Bergmann F and Ungar H (1960) The enzymatic oxidation of 6-mercaptopurine to 6-thiouric acid. *J Am Chem Soc* **82**:3957–3960.
- Burchenal JH, Murphy ML, Ellison RR, Sykes MP, Tan TC, Leone LA, Karnofsky DA, Craver LF, Dargeon HW, and Rhoads CP (1953) Clinical evaluation of a new antimetabolite, 6-mercaptopurine, in the treatment of leukemia and allied diseases. *Blood* **8**:965–999.
- Cao H, Pauff JM, and Hille R (2010) Substrate orientation and catalytic specificity in the action of xanthine oxidase: the sequential hydroxylation of hypoxanthine to uric acid. *J Biol Chem* **285**:28044–28053.
- Choughule KV, Barr JT, and Jones JP (2013) Evaluation of rhesus monkey and guinea pig hepatic cytosol fractions as models for human aldehyde oxidase. *Drug Metab Dispos* **41**:1852–1858.
- Dalvie D, Xiang C, Kang P, and Zhou S (2013) Interspecies variation in the metabolism of zonisipride by aldehyde oxidase. *Xenobiotica* **43**:399–408.
- Elion GB (1967) Symposium on immunosuppressive drugs. Biochemistry and pharmacology of purine analogues. *Fed Proc* **26**:898–904.
- Garattini E and Terao M (2012) The role of aldehyde oxidase in drug metabolism. *Expert Opin Drug Metab Toxicol* **8**:487–503.
- Garattini E, Mendel R, Romão MJ, Wright R, and Terao M (2003) Mammalian molybdo-flavoenzymes, an expanding family of proteins: structure, genetics, regulation, function and pathophysiology. *Biochem J* **372**:15–32.
- Giverhaug T, Loennechen T, and Aarbakke J (1999) The interaction of 6-mercaptopurine (6-MP) and methotrexate (MTX). *Gen Pharmacol* **33**:341–346.
- Hall WW and Krenitsky TA (1986) Aldehyde oxidase from rabbit liver: specificity toward purines and their analogs. *Arch Biochem Biophys* **251**:36–46.
- Harrison R (2002) Structure and function of xanthine oxidoreductase: where are we now? *Free Radic Biol Med* **33**:774–797.
- Hutzler JM and Tracy TS (2002) Atypical kinetic profiles in drug metabolism reactions. *Drug Metab Dispos* **30**:355–362.
- Keuzenkamp-Jansen CW, van Baal JM, De Abreu RA, de Jong JG, Zuiderent R, and Trijbels JM (1996) Detection and identification of 6-methylmercapto-8-hydroxypurine, a major metabolite of 6-mercaptopurine, in plasma during intravenous administration. *Clin Chem* **42**:380–386.
- Krenitsky TA, Neil SM, Elion GB, and Hitchings GH (1972) A comparison of the specificities of xanthine oxidase and aldehyde oxidase. *Arch Biochem Biophys* **150**:585–599.
- Nielsen OH, Vainer B, and Rask-Madsen J (2001) Review article: the treatment of inflammatory bowel disease with 6-mercaptopurine or azathioprine. *Aliment Pharmacol Ther* **15**:1699–1708.
- Obach RS (2004) Potent inhibition of human liver aldehyde oxidase by raloxifene. *Drug Metab Dispos* **32**:89–97.
- Rashidi MR, Beedham C, Smith JS, and Davaran S (2007) In vitro study of 6-mercaptopurine oxidation catalysed by aldehyde oxidase and xanthine oxidase. *Drug Metab Pharmacokinet* **22**:299–306.
- Rowland K, Lennard L, and Lilleyman JS (1999) In vitro metabolism of 6-mercaptopurine by human liver cytosol. *Xenobiotica* **29**:615–628.
- Sahi J, Khan KK, and Black CB (2008) Aldehyde oxidase activity and inhibition in hepatocytes and cytosolic fractions from mouse, rat, monkey and human. *Drug Metab Lett* **2**(3):176–183.
- Segel I (1993) Kinetics of unireactant enzymes, in *Enzyme Kinetics* (Segal I ed.) pp 18–98, John Wiley & Sons, New York.
- Van Scoik KG, Johnson CA, and Porter WR (1985) The pharmacology and metabolism of the thiopurine drugs 6-mercaptopurine and azathioprine. *Drug Metab Rev* **16**:157–174.
- Weidert ER, Schoenborn SO, Cantu-Medellin N, Choughule KV, Jones JP, and Kelley EE (2014) Inhibition of xanthine oxidase by the aldehyde oxidase inhibitor raloxifene: implications for identifying molybdopterine nitrite reductases. *Nitric Oxide* **37**:41–45.
- Zimm S, Grygiel JJ, Strong JM, Monks TJ, and Poplack DG (1984) Identification of 6-mercaptopurine riboside in patients receiving 6-mercaptopurine as a prolonged intravenous infusion. *Biochem Pharmacol* **33**:4089–4092.

Address correspondence to: Dr. Jeffrey P. Jones, Department of Chemistry, Washington State University, P.O. Box 644630, Pullman, WA 99164-4630. E-mail: jpj@wsu.edu
